UNIVERSITÀ
DI PAVIA

PhD IN BIOMEDICAL SCIENCES

DEPARTMENT OF BRAIN AND BEHAVIORAL SCIENCES

UNIT OF NEUROPHYSIOLOGY

Neuroimaging and clinical spectrum of sporadic cerebral amyloid angiopathy

PhD Tutor: Prof. Alfredo Costa

PhD dissertation of
Giulia Perini

a.a. 2021/2022

Contents

Chapter 1: Introduction

1.1 Epidemiology

The term cerebral amyloid angiopathy (CAA) describes an heterogeneous group of biochemically and genetically various central nervous system (CNS) disorders, which share a characteristic morphological finding on pathological examination, i.e. amyloid fibrils deposited in the walls of small to medium-sized, blood vessels, mostly arterial [1–5]. CAA is classified into several types according to the amyloid protein involved. So far, seven amyloid proteins have been reported in CAA, including amyloid β-protein (Aβ), cystatin C (ACys), prion protein (APrP), ABri/ADan, transthyretin (ATTR), gelsolin (AGel), and immunoglobulin light chain amyloid (AL) [3]. CAA mostly occurs in a sporadic form in the elderly, while rare familial forms occur in younger patients and generally lead to more severe clinical manifestations [1]. The sporadic form and most hereditary forms of CAA are of the amyloid-β (Aβ-CAA) type [1].

From a historical perspective, vascular Aβ deposition in the CNS was first described by Gustav Oppenheim in 1909, who found foci of necrosis in the brain parenchyma adjacent to hyalinized capillary walls in brains of autopsied individuals with senile dementia [6]. In 1938, Scholz published the first article focusing solely on cerebral vascular abnormalities now recognized as CAA [7]. The observation that CAA is limited to the vascular media without adjacent parenchymal involvement was made in 1954 by Stefanos Pantelakis, together with the observations of the main involvement of small to medium-sized, cortical and leptomeningeal blood vessels, preferentially of posterior brain regions [8]. Moreover, Pantelakis observed the strong association of CAA with age and dementia, the lack of association with hypertension and atherosclerosis and the lack of connections with systemic amyloidosis [8]. Okazaki and colleagues in 1979 clarified the relationship between CAA and lobar intracerebral hemorrhage (ICH) [9]. Finally, in 1984 Aβ was isolated from cerebral blood vessels by Glenner and Wong [10].

Sporadic CAA is a small vessel disease (SVD) characterized by the Aβ peptide deposition in the walls of cortical and leptomeningeal arteries, arterioles and capillaries [2]. CAA occurs frequently in elderly people and it is a common and important cause of symptomatic lobar ICH, cognitive impairment (either chronic or rapidly progressive) or transient focal neurologic symptoms [2,5,11]. The prevalence of CAA in the elderlies is

28-38% in not demented and 55-59% in demented patients in population-based autopsy studies [12]. Moreover, more than 90% of Alzheimer's disease (AD) patients show he presence of CAA in autopsy studies [13], but only 25% have moderate-severe CAA [14]. The most important risk factor for CAA development is age, while the ApoE ε4 and ε2 alleles are the only genetic risk factors robustly associated with the risk of developing sporadic CAA [15].

Familial forms of CAA are exceedingly rare autosomal dominant disorders related to genetic variants of Aβ or to non-Aβ proteins, which provide unique paradigms to examine the role of amyloid in the mechanism of disease pathogenesis [16]. Among familiar Aβ cerebral amyloidosis, most mutations are reported within the Aβ region comprising residues 21–23 [16]. The first discovered and best characterized form is hereditary cerebral hemorrhage with amyloidosis Dutch-type, which is clinically defined by recurrent strokes, vascular dementia and fatal cerebral bleeding in the fifth to sixth decades of life (AβE22Q mutation) [17]. Within the same amino acid cluster, the Italian type variant is responsible of a 10- to 20-year progression of recurrent strokes and mild cognitive decline (AβE22K mutation) [18]. Among non-Aβ cerebral amyloidosis, hereditary cerebral hemorrhage with amyloidosis Icelandic type is a cystatin C-related cerebral amyloidosis causing cerebral hemorrhage with fatal outcome in the third to fourth decade of life in approximately half of the cases [16].

1.2 Pathophysiology

Aβ is proteolytically cleaved by β- and γ-secretase from its precursor, β-amyloid precursor protein (APP) (Figure 1) [19]. In contrast to Aβ deposition in AD, a substantial proportion of Aβ in vascular deposits is the shorter Aβ 1-40 species, which is more soluble than the longer Aβ 1-42 more prominent in the plaques in brain tissue [2]. Soluble Aβ forms undergo a change in conformation (via mechanisms that remains largely unknown) resulting in a predominantly β-sheet structure, highly prone to oligomerization, fibrillization and deposition [1]. In turn, these deposits trigger a secondary cascade of events including, among others, release of inflammatory components, activation of the complement system, oxidative stress, alteration of the blood-brain barrier (BBB) permeability, and cell toxicity [1].

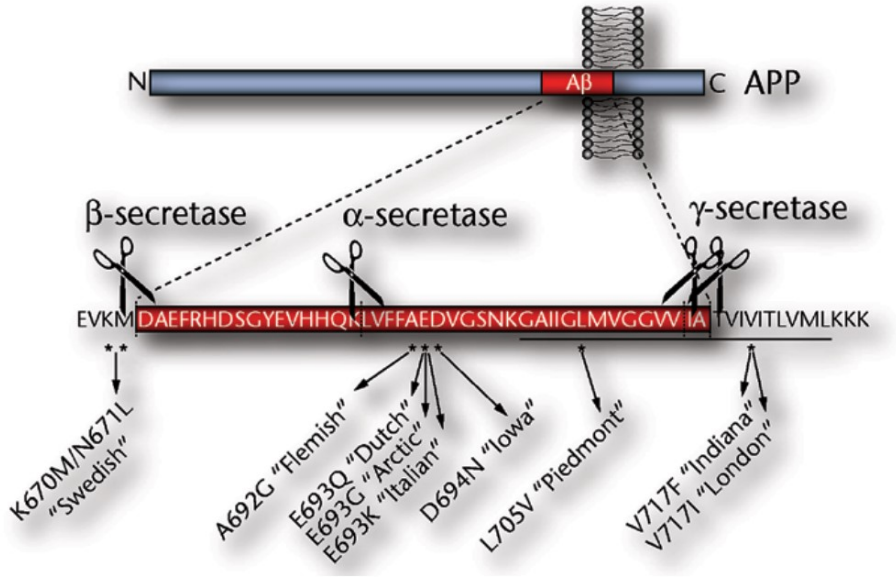

Figure 1 APP, the secretase cleavage sites, and the location of APP mutations causing familial AD and/or Aβ-CAA are shown. APP is in blue, the amino acid sequence of Aβ1-42 (boxed) is shown in red, and the predicted transmembrane domain of APP is underscored. The major cleavage sites for α-, β-, and γ-secretases are indicated by the scissors. The location of the most important APP mutations known to cause either familial AD and/or Aβ-CAA are marked by asterisks. From Herzig et al., Brain Pathol 2006 [19]

Vascular amyloid has been suggested to be predominantly generated by neurons and subsequently deposited in the vessel wall [19]. Since no evidence of increased Aβ production has been found in sporadic CAA, imbalance between Aβ production and clearance is generally considered a key element in the formation of amyloid deposits [1]. Mechanisms of Aβ clearance involve the drainage to blood flow with interstitial fluid along perivascular spaces as well as the actively translocation through the BBB into the blood (Figure 2) [19]. Changes of the vessel wall properties, i.e. thickening of the basement membrane caused by perivascular astrocytosis in response to overproduction of TGF-β1, might impair the interstitial fluid clearance evidenced by several basement membrane components that have been shown to bind Aβ directly or indirectly through the ApoE [19]. On the other hand, the amphyphilic nature of Aβ precludes its crossing through the BBB unless mediated by specialized carriers and/or

receptor transport mechanisms; among receptors involved, the upregulation of the lipoprotein receptor (LRP) in vascular smooth muscle accelerates Aβ vascular deposition [19].

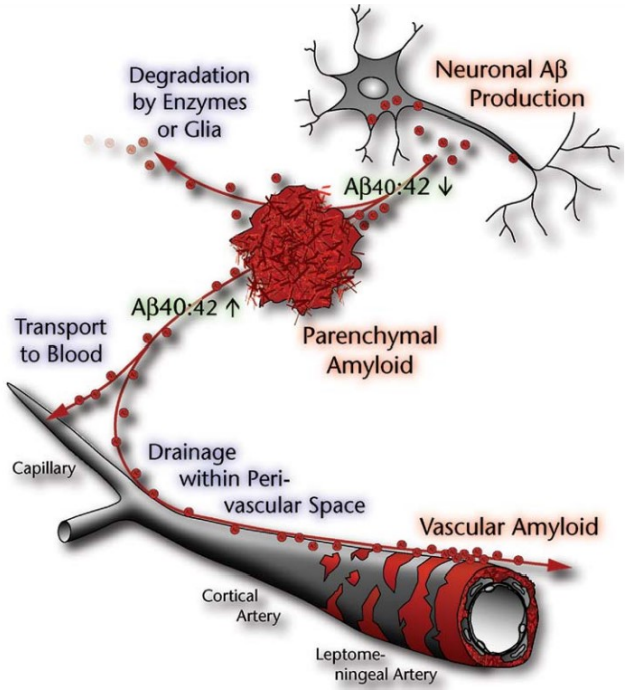

Figure 2 Hypothetical mechanism involved in Aβ-CAA formation. Neuronally produced Aβ is transported via interstitial fluid to the blood vessels. On its way it is cleared by Aβ-degrading enzymes and/or glia cells. At the vasculature Aβ is cleared by receptor-mediated translocation through the BBB into the blood, or by perivascular drainage. If these clearance mechanisms are impaired, Aβ accumulates and forms amyloid deposits either in the brain parenchyma (amyloid plaques) or in the vessel wall (vascular amyloid). Thereby, a low Aβ40:42 ratio of soluble Aβ favors parenchymal amyloid, ie, Aβ accumulates close to the site of its production, while a high Aβ40:42 ratio promotes vascular amyloid. From Herzig et al., Brain Pathol 2006 [19]

Aβ deposition leads to important modification of structures and vascular functions. Pathological examination of blood vessels in both sporadic and familial CAA show loss of smooth muscle cells, vessel wall thickening, lumenal narrowing, concentric splitting of the vessel wall, microaneurysm formation, and perivascular microhemorrhage [2].

Two specific pathological subtypes are described: CAA type 1, characterized by Aβ deposition in cortical capillaries (with or without involvement of other vessels), and CAA type 2, where Aβ deposits are restricted to leptomeningeal and cortical arteries, but not capillaries [20]. CAA type 2 is associated with primarily hemorrhagic lesions [lobar intracerebral macrohemorrhage, cortical microhemorrhage, and cortical superficial siderosis (cSS)/focal convexity subarachnoid hemorrhage (SAH)], while CAA type 1 with primarily ischemic lesions (cortical infarction and ischemic changes of the white matter) and coexistence with AD pathology [5]. An emergent pathological-clinical CAA manifestation is a subacute leukoencephalopathy caused by CAA-related inflammation/angiitis [3]. Thus, CAA-related hemorrhagic, ischemic and inflammatory alterations are associated with the risk of stroke, dementia, and encephalopathies [3,5].

1.3 Clinical features

Symptomatic intracerebral hemorrhage

CAA-related ICH is the second most common cause of ICH following hypertensive angiopathy, accounting for at least 5–20 % of all spontaneous ICH according to clinicopathological studies [2]. CAA is significantly associated with lobar ICH, especially temporal and occipital lobe, rarely cerebellum or deep structures, reflecting the localization of the underlying microangiopathy (sporadic Aβ-CAA is commonly found in the meningeal and cortical vessels of cerebral cortices) [3]. The predilection for the occipital lobes is not well understood but one hypothesis is that greater tortuosity of occipital small arteries impairs perivascular drainage [21]. By contrast, hypertensive-related ICH is associated with deep or infratentorial regions (basal ganglia, thalamus, pons) as a consequence of hypertensive arteriopathy which causes lipohyalinosis and fibrinoid necrosis of small lenticulostriate perforating arteries. CAA with symptomatic lobar ICH present less neurofibrillary tangles and more APOE ε2 phenotype and disseminated CSS, than CAA without ICH [22]. CAA-related lobar ICH is often multiple and recurrent (at a rate of recurrence on the order of 10% per year) [5].

Cognitive impairment and dementia

Cognitive impairment in CAA was first reported over two decades ago and is associated with SVD pathology (hemorrhagic/ischemic vascular lesions) with the eventually

contribution of AD pathology [3,5]. Dementia was reported in 74% of individuals with severe CAA at autopsy and in clinical settings it can precede ICH, thus occuring independently of symptomatic ICH [3,5]. Dissecting the independent impact of SVD and AD pathology in CAA-related cognitive decline is still an open issue. Neuropathological studies suggest that vascular and parenchymal Aβ deposits can occur either relatively independently of each other, or can overlap: individuals who die of CAA-related hemorrhage, approximately 50% meet AD criteria, while approximately 25% of patients with AD also have severe CAA [2]. Neuroimaging evidence further supports these neuropathological findings: in particular lobar cerebral microbleeds (CMB), a hallmark feature of CAA, are detectable in ⅓ or more of patients diagnosed with AD and are more considerably more prevalent in AD compared to healthy population and other causes of neurodegenerative dementia [2]. Interactive effects of neurodegenerative and cerebrovascular diseases on cognition certainly result from the cumulative brain injuries caused by each process, but also from the crosstalk between the two processes [4]. Cognitive impairment in CAA seems to correlate most directly with non-haemorrhagic SVD markers, namely white matter hyperintensities (WMH), cerebral microinfarcts and in particular structural disconnection measured with diffusion tensor imaging (DTI), suggesting that disconnection has a primary role in vascular cognitive impairment and dementia [4]. Vascular dysfunction caused by CAA reduces perivascular Aβ clearance, thus creating a vicious cycle of vascular and parenchymal Aβ accumulation (cerebrovascular dysfunction is in fact an early step also in AD pathogenesis) [4]. Finally, tau deposition has been observed around Aβ-laden vessels in sporadic and hereditary CAA and brain atrophy is recognized to be feature of CAA [4].

Rapidly progressive cognitive and neurological decline (CAA related inflammation)

CAA can rarely present as a spontaneous acute/subacute encephalopathy namely cerebral amyloid angiopathy-related inflammation (CAA-ri), characterized by the presentation of neurological symptoms that vary from very mild cognitive disturbances and headaches to rapidly progressive cognitive decline, seizures, focal neurological deficits and impaired consciousness [23–25]. Typical magnetic Resonance Imaging (MRI) findings are acute WMHs suggestive of vasogenic edema (VE), associated with MRI hallmarks of CAA such as CMBs and cSS [25]. In the recent past, CAA-ri has

generated additional interest for its clinic-radiological similarities to the amyloid-related imaging abnormalities (ARIA), developed by a subset of patients with AD receiving bapineuzumab and other anti-amyloid drugs, such as avagacestat and gantenerumab [26]. Therapies using anti-Aβ antibodies might be complicated by ARIA-E (edema), consisting of focal areas of WMH suggestive of parenchymal edema and/or effusion, or ARIA-H (hemorrhage), consisting of CMBs and cSS [27]. The pathogenetic mechanism of ARIA is still unknown, but it is supposed to be an abnormal immune response directed toward the deposited cerebrovascular Aβ, modulated by antibody dosage, which is suggestive of a specific role of the anti-Aβ antibodies administered for therapeutic purposes [27].

Transient neurological symptoms (Amyloid spells)

An increasingly recognized presentation of CAA consists of transient focal neurological episodes (TFNE), sometimes less specifically referred to as amyloid spells, which include predominantly positive symptoms ("aura-like") and predominantly negative symptoms ("transient ischemic attack–like") [5,28]. TFNE were found to occur in 14% of patients with CAA and are mostly recurrent, stereotyped, and brief (usually <30 minutes) [28]. The clinical features of the episodes indicate a cortical rather than a subcortical origin and are often associated with hemorrhagic MRI lesions, including SAH and cSS [5]. Thus, TFNE are probably related to the hemorrhagic rather than the ischemic components of CAA; possible mechanisms include focal seizure-like activity or migraine aura-like cortical spreading depression [28]. A strikingly high early risk of symptomatic lobar ICH (37.5% at 2 months) after CAA-related TFNE is reported [28].

1.4 Diagnosis and biomarkers

CAA is defined by the histopathologic deposition of Aβ in the cerebrovasculature and through the 1980s the disorder was only diagnosed in patients with available brain tissue from hematoma evacuation, biopsy, or most commonly post-mortem exam [29]. Introduction of the imaging-based Boston criteria for diagnosis of CAA in the 1990s, allowed in vivo diagnosis of CAA and substantially moved the field from the pathologist's realm to the clinician's [30]. Probable or possible CAA diagnosis is based on brain imaging plus clinical exclusions (Table 1). CAA entailed neuroimaging

demonstration hemorrhages restricted to lobar brain regions, defined as cerebral cortex, corticosubcortical junction and subcortical white matter; the incorporation of cSS as one additional hemorrhagic lesion ("modified Boston criteria"), was proposed and validated in 2010 [31]. MRI-histopathological studies of patients presenting primarily with ICH have provided validating evidence for the original Boston criteria probable CAA diagnosis (sensitivities ranging from 57.9% to 76.9% and specificities of 87.5% to 100%), while the modified Boston Criteria improved sensitivity without lowering specificity [29,31,32]. Among non-ICH individuals with other clinical presentations such as cognitive impairment or transient focal neurological episodes, it was detected a lower sensitivity of 42.4% and similar specificity of 90.9% [29,33].

Table 1, Classic and *modified* Boston criteria for diagnosis of CAA.

1. Definite CAA Full post-mortem examination demonstrating: • Lobar, cortical, or cortical-subcortical haemorrhage • Severe CAA with vasculopathy • Absence of other diagnostic lesion
2. Probable CAA with supporting pathology Clinical data and pathologic tissue (evacuated haematoma or cortical biopsy) demonstrating: • Lobar, cortical, or cortical-subcortical haemorrhage • Some degree of CAA in specimen • Absence of other diagnostic lesion
3. Probable CAA Clinical data and MRI or CT demonstrating: • Multiple haemorrhages restricted to lobar, cortical, or cortical-subcortical regions (cerebellar haemorrhage allowed) **OR** • *Single lobar, cortical, or cortical-subcortical haemorrhage and focal[b] or disseminated[c] superficial siderosis* • Age≥55 years • Absence of other cause of haemorrhage[a]

4. Possible CAA
Clinical data and MRI or CT demonstrating:
• Single lobar, cortical, or cortical-subcortical haemorrhage **OR**
• *Focal[b] or disseminated[c] superficial siderosis*
• Age ≥55 years
• Absence of other cause of haemorrhage[a]
[a] **Other causes of haemorrhage include:** antecedent head trauma, haemorrhagic transformation of an ischemic stroke, arteriovenous malformation, haemorrhagic tumour, warfarin therapy with international normalisation ratio > 3 and vasculitis
[b] **Focal siderosis: siderosis:** siderosis restricted to 3 or fewer sulci.
[c] **Disseminated siderosis:** siderosis affecting at least 4 sulci

Similarly, a definite diagnosis of CAA-ri requires histopathologic confirmation; however in the presence of an appropriate clinical presentation, MRI WMH patterns asymmetric and extended to the immediately subcortical white matter (probable CAA-ri) or simply extended to the immediately subcortical white matter (possible CAA-ri) and at least one corticosubcortical hemorrhagic lesion meet clinical-radiological criteria of CAA-ri (Table 2) [25]. MRI-histopathological studies found a sensitivity and specificity of 82% and 97%, respectively, for the probable criteria and a sensitivity and specificity of 82% and 68%, respectively, for the possible criteria [25].

Table 2, Criteria for the diagnosis of CAA-ri.

1. Probable CAA-ri
• Age ≥40 years
• Presence of ≥1 of the following clinical features: headache, decrease in consciousness, behavioral change, or focal neurological signs and seizures; the presentation is not directly attributable to an acute ICH
• MRI shows unifocal or multifocal WMH lesions (corticosubcortical or deep) that are asymmetric and extend to the immediately subcortical white matter; the asymmetry is not due to past ICH
• Presence of ≥1 of the following corticosubcortical hemorrhagic lesions: cerebral macrobleed, cerebral

microbleed, or cortical superficial siderosis • Absence of neoplastic, infectious, or other cause
1. Possible CAA-ri • Age ≥40 years • Presence of ≥1 of the following clinical features: headache, decrease in consciousness, behavioral change, or focal neurological signs and seizures; the presentation is not directly attributable to an acute ICH • MRI shows WMH lesions that extend to the immediately subcortical white matter • Presence of ≥1 of the following corticosubcortical hemorrhagic lesions: cerebralmacrobleed, cerebral microbleed, or cortical superficial siderosis • Absence of neoplastic, infectious, or other cause

Neuroimaging

In vivo diagnosis of CAA is based on clinical data and MRI findings; lobar, cortical or cortical-subcortical hemorrhages (including ICH and CMBs) and focal or disseminated cSS are the hallmark biomarkers for CAA. Other common MRI findings are WMHs, cerebral microinfarcts, enlarged perivascular spaces (EPVS) and cortical atrophy (Figure 3). In the past years, the broader availability of brain MRI, allowed the better characterization of the expanding imaging spectrum of CAA and the assumption that neuroimaging markers may reflect distinct but related aspects of CAA pathophysiology (Table 3) [34].

CMBs are small round or ovoid lesions detected in hyposignal on paramagnetic sensitive MRI sequences including T2*-weighted gradient-recalled echo (T2*GRE) or susceptibility-weighted (SWI) [35]. Pathological studies showed that CMBs correspond to focal accumulations of hemosiderin-laden macrophages adjacent to abnormal small vessels affected by hypertensive angiopathy or CAA [36]. The topography of CMB distribution has been considered as an important marker for underlying cerebral SVD. Association of deep and infratentorial CMBs with hypertensive arteriopathy and lobar, cortical or cortical-subcortical CMBs with CAA has been demonstrated with histopathological studies and preliminary amyloid positron emission tomography (PET) investigations [37]. Also, strictly lobar microbleeds are associated with APOE epsilon 4;

in contrast, cardiovascular risk factors and presence of lacunar infarcts and WMHs are associated with deep or infratentorial microbleeds [38]. It has been shown that lobar CMBs can be used as a diagnostic marker for CAA in hospital-based populations with a positive predictive value reaching >85%; however, the positive predictive value dropped to 25% in the general population, suggesting that lobar CMBs may be a more accurate CAA marker in patients with related clinical symptoms [39]. The detection of CMBs is associated with important clinical aspects. Presence of CMBs is associated with both risk of ICH and ischemic stroke [40]. In contrast, the effects of CMBs on cognitive function is less conclusive. Although not associated with the risk of dementia in the overall population, the presence of CMBs has been associated with several types of cognitive dysfunction and evidence suggests that CMBs in lobar regions, which are usually attributed to CAA, are most strongly associated with cognitive decline [5,40,41].
cSS refers to the curvilinear, homogeneous hypointense lesion that follows the gyral cortical surface and can be demonstrated on blood-sensitive MRI sequences [39]. This lesion may have a 'track-like' appearance that results from hemosiderin accumulating at bilateral sides of cortical sulcus in subacute and chronic stages of cSAH [39]. According to the involved areas, cSS could be divided into focal and disseminated types. cSS should be differentiated from 'classical' superficial siderosis, which predominantly affect infratentorial areas [42]. cSS is considered a specific marker of CAA, evident in 40 to 60% of CAA patients [39]. cSS is associated with TFNEs and might be a marker of future ICH risk in CAA patients [5,43].
WMHs refer to bilateral, mostly symmetrical, white matter hyperintense lesions demonstrated on T2-weighted imaging study with corresponding iso- or hypointense appearance on T1-weighted sequence [39]. The pathophysiology in WMH is probably associated to chronic ischemic changes, brain tissue damage, BBB disruption, decreased vascular integrity, and interference with capillary permeability [39]. The topography of WMH distribution is considered as an important marker for different type of underlying SVD. Peri-basal ganglia lesions are more often associated with hypertensive vasculopathy, frontal or equally distributed WMHs were the most common pattern in healthy elderly, while subcortical and posterior predominant WMHs are associated with CAA [3,39]. Presence of WMHs is associated a great variety of clinical disfunctions,

from risk of ischemic stroke and ICH to dementia, both in general population and CAA patients [5,39,40,44].

Cortical microinfarcts are hyperintense lesions with greatest dimension less than 5mm on high resolution T2-weighted imaging studies (3- and 7-Tesla MRI) that are located within the cortical ribbon [39]. Microinfarcts are associated with both risk of ischemic stroke and ICH in the overall population and with dementia in CAA cohort [3,5,40].

EPVSs are MRI-visible linear or dot-like structures depending on the different imaging angle with the vessels, hyperintense on T2-weighted sequences similar to cerebrospinal fluid (CSF) [39]. PVSs (also known as Virchow–Robin spaces) represent extensions of subarachnoid spaces that surround small penetrating cortical arterioles and venules as they run from brain surfaces into brain parenchyma, draining CSF to ventricles, with a clearance function that include Aβ [39]. Like other SVD imaging features, EPVS topography reflects different underlying pathology; those in the centrum semiovale are CAA-related while those in the basal ganglia are linked to hypertensive vasculopathy [39,45]. EPVSs are present in almost all patients with spontaneous ICH and are associated with dementia in CAA patients [5,45].

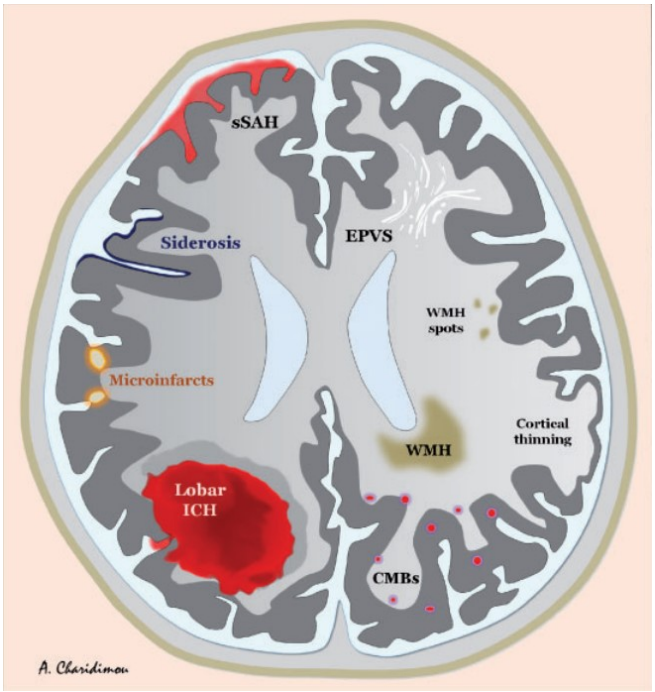

Figure 3 Schematic representation of the spectrum of haemorrhagic and ischaemic manifestations of sporadic CAA, visible on structural MRI. From Charidimou et al., Brain 2017 [5]

Table 3, Association of MRI markers of SVD with risk of ICH and dementia in the overall population [40] and in CAA patients [5].

SVD MRI markers		ICH	Dementia
CMBs	Overall	xxx	NS
	CAA*	xxx	xx
cSS	Overall		
	CAA*	xx	NS
WMH	Overall	xx	xxx
	CAA*	xxx	xx
EPVS	Overall		
	CAA*	xxx	xx
Microinfarcts	Overall	xxx	NS
	CAA*	NS	xxx

CMBs, cerebral microbleeds; cSS, cortical superficial siderosis; WMH, white matter hyperintensities; EPSV, enlarged perivascular spaces; NS, not significant. * for CAA only SVD MRI markers located in cortical or cortical-subcortical regions are considered

Amyloid biomarkers

While MRI is commonly used for diagnosis within the validated Boston criteria, this approach is limited in detecting the pathologic consequences of rather advanced CAA [5]. Direct and early markers of cerebrovascular amyloid in vivo remain a key unmet need in the field; pathophysiologic biomarker would indeed have clinical implications for accurate early diagnosis, dementia and stroke risk stroke risk classification and future therapeutic strategies [46]. The clinical usefulness of these biomarkers in everyday practice currently remains limited and under investigation [5].

Amyloid PET imaging has been shown to measure the burden and location of β-amyloid deposit, however due to the low resolution of PET, vascular amyloid cannot be differentiated from parenchymal amyloid [46–48]. The sensitivity of amyloid PET for

CAA diagnosis ranged from 60% to 91% and the specificity from 56% to 90% [46]. The main limitation is represented by the possibility of a proportion of elderly healthy subjects and patients with deep ICH having incipient AD or CAA pathology [47,48]. However, in the appropriate clinical setting, it would be useful in differentiating patients with probable CAA from cognitively normal healthy controls or patients with deep ICH, mainly because a negative scan almost certainly rules out advanced CAA [46]. Future directions for differential diagnosis between CAA and AD include the assessment of the regional PET uptake pattern and perhaps early-phase PET images [47]. In a research setting, amyloid PET has been demonstrated to show CAA-related microbleeds [5,47].

With regard to CSF analyses, the direct measurement of amyloid proteins and other protein markers suggests that measurement of beta-amyloid 1-40 (Aβ40), beta-amyloid 1-42 (Aβ42), total tau (t-tau), and phosphorylated tau (p-tau) might differentiate CAA from controls as well as from AD patients [49,50]. In particular the Aβ40/42 ratio, but also elevated p-tau and t-tau, differentiates between AD and CAA, however without clinically useful accuracy [50]. Similarly for CAA-ri, outside the diagnostic criteria, CSF abnormalities such as mildly elevated protein and the presence of leukocytes have been suggested to be useful for the diagnosis, however neither sensitive nor specific [25]. Most intriguingly, elevated CSF anti–β-amyloid autoantibodies during the acute phase of CAA-ri and not in noninflammatory CAA or other non-CAA inflammatory disorders have been detected, but validation of experimental cutoff values for CAA-ri diagnostic confirmation is needed [27].

Chapter 2: Experimental Study 1

2.1 Aim

To clarify whether neuroimaging markers differ between patients with CAA with hemorrhagic versus cognitive onset. In addition, exploratory analyses investigated whether neuroimaging markers are associated with specific CSF or neuropsychological profiles in the cognitive onset group.

2.2 Materials and Methods

2.2.1 Study design and participants

The study was designed as a single-site retrospective study. We assessed 90 patients with a diagnosis of CAA according to the modified Boston criteria [32] attending the C. Mondino National Neurological Institute in Pavia, Italy, over a nine-year period (2012 to 2021) (Figure 4). Based on their clinical presentation, patients had been initially referred to the Memory Clinic or the Stroke Unit. We evaluated all patients with suspected CAA. i.e., patients with cognitive decline, survivors of spontaneous lobar ICH, patients with CAA-related inflammation, and those who, during investigation for other symptoms, had been found to have features characteristic of CAA, such as lobar CMBs, cSS and asymptomatic lobar ICH. The patient inclusion criteria were: (1) fulfilment of the modified Boston criteria for probable or possible CAA [32]; (2) availability of 3 or 1.5 Tesla MRI sequences including T2*-weighted gradient-recalled echo (T2*-GRE), fluid attenuated inversion recovery (FLAIR), T2-weighted TSE, and 3D T1-weighted MPRAGE; (3) availability of clinical data. CAA patients without an adequate MRI imaging workup were excluded (n=25). Clinical data and medical history at the time of symptom onset (age, gender, family history, clinical history, vascular risk factors including hypertension, diabetes, dyslipidemia, use of antithrombotic drugs, anticoagulants, other drugs) were obtained from medical records. Patients were then classified into two groups based on the presentation of the disease at onset: hemorrhagic or cognitive. Patients who presented with a transient focal neurological episode as first symptom were excluded because they could not be assigned to either of the two main study groups (n=4). Finally, a total of 61 patients (31 with hemorrhagic onset of CAA and 30 with cognitive onset) were included in this study.

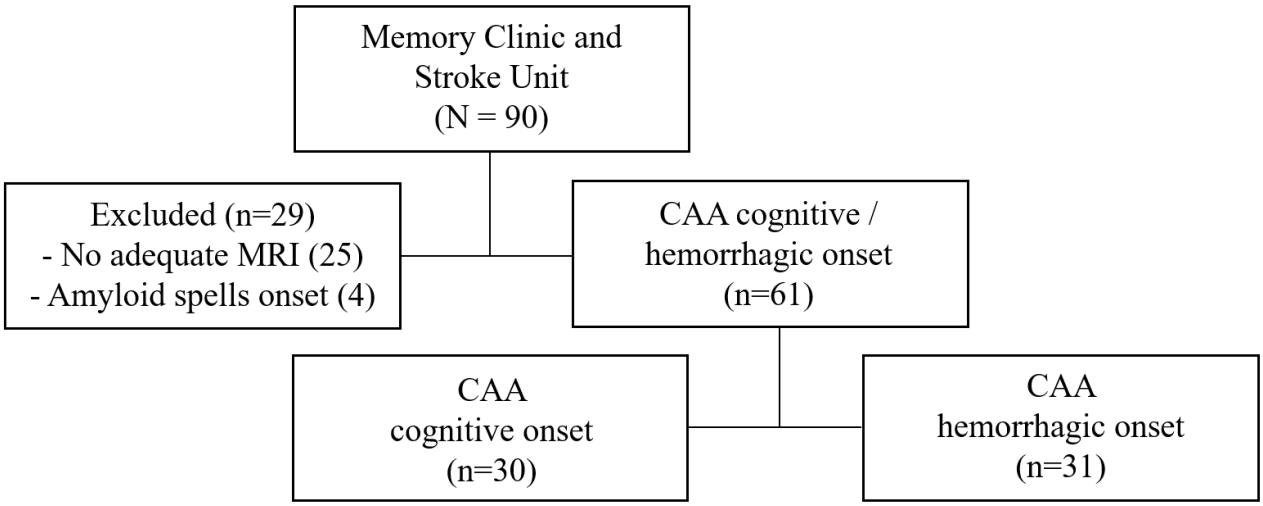

Figure 4 Flowchart illustrating the selection of the study participants. Study participants were selected from a larger study cohort (N=90), recruited at a Memory Clinic and a Stroke Unit. Twenty-five participants did not meet the MRI investigation criteria designed for the present study protocol; 4 participants presented with amyloid spells onset and were thus excluded.

2.2.2 Biomarkers

Neuroimaging

For the purposes of this study, we analyzed: 2D T2*-weighted GRE to evaluate lobar hemorrhages, CMBs, and cSS; 3D T2-weighted FLAIR to evaluate WMHs and cortical microinfarcts; 2D T2-weighted TSE to evaluate EPVS; and 3D T1-weighted MPRAGE to evaluate brain atrophy. Image sequences were acquired using a 3T Magnetom Skyra scanner (Siemens Healthcare, Erlangen, Germany) with a 32-channel receive head coil (n=28) or a 1.5T Philips scanner (Philips Gyroscan, Koninklijke, The Netherlands) with a 20-channel head coil (n=33). Visual atrophy scales were applied by an expert rater with more than two years' experience in visual atrophy rating. All scores were formulated prior to the analyses, and blinded to all clinical data and medical history.

Cerebral microbleeds were scored in line with the STRIVE (STandards for ReportIng Vascular changes on nEuroimaging) recommendations [51]. Lobar CMBs (presence and number) were evaluated on axial T2*-GRE images using current consensus criteria [35] and categorized by number and location according to the Microbleed Anatomical Rating Scale [52]. Number of CMBs was categorized as: 0 to 3; 4 to 10; and more than 10

CMBs, while location of CMBs was evaluated considering the following sites: frontal lobe, temporal lobe, parietal lobe, occipital lobe, insular lobe, and infratentorial regions.

Cortical superficial siderosis was evaluated on axial T2*-GRE sequences and number of cSS was categorized as: 0; 1; and more than 1 cSS. cSS were also scored using the multifocality rating scale [53], which scores each hemisphere (right-left) separately: 0 denotes no cSS; 1 denotes one sulcus or up to three immediately adjacent sulci with cSS; and 2 denotes two or more non-adjacent sulci or more than three adjacent sulci with cSS. The total cSS multifocality score is calculated by adding the right and left hemisphere scores (range 0-4).

Total white matter hyperintensities were assessed using the four-point Fazekas scale [54], according to which the degree of white matter changes on axial T2-weighted FLAIR images was rated as: grade 0, indicating no or occasional punctate white matter changes; grade 1, multiple punctate white matter changes; grade 2, incipient confluence or bridging of punctate changes; grade 3, confluent white matter changes.

Enlarged perivascular spaces in the centrum semiovale (CSO-PVS) and in the basal ganglia (BG-PVS) were evaluated on axial T2-weighted and FLAIR sequences using a single predefined slice (the first slice above the anterior commissure for the basal ganglia, and the first slice above the level of the lateral ventricles for the centrum semiovale).

Cortical microinfarcts were detected in FLAIR sequences.

Medial temporal lobe atrophy (MTA), posterior atrophy (PA), and global cortical atrophy-frontal (GCA-F) scales were applied on 3D T1-weighted MR images in both hemispheres, according to the original descriptions [55–57]. The MTA scale assesses the width of the choroid fissure and the temporal horn, as well as the height of the hippocampus; the PA scale assesses the width of the posterior cingulate and parieto-occipital sulci, and atrophy of the parietal lobe and precuneus; and the GCA-F scale evaluates the severity of frontal lobe atrophy.

CSF and neuropsychological assessment

Twenty participants underwent a lumbar puncture at the level of the L3/L4 or L4/L5 intervertebral space, performed in accordance with our Institute's standard protocol for patients with cognitive disorders. CSF samples were centrifuged for 10 min at 1,800 g at 4°C within 3 h of collection. The samples were then divided into aliquots of 0.5 ml

and stored in polypropylene tubes at −80°C. Measurement of CSF levels of Aβ42, t-tau, and p-tau was performed using chemiluminescence enzyme immunoassay (Lumipulse G600II, Fujirebio); measurement of Aβ40 was performed in only seven subjects, due to the relatively recent introduction of this assay in our laboratory. Biomarker profile was considered suggestive of AD pathology if Aβ42 < 599 pg/ml, t-tau > 404 pg/ml, p-tau > 56.5 pg/ml, Aβ42/t-tau < 1.27, Aβ42/p-tau < 8.10, and Aβ42/Aβ40 < 0.069 [58,59].

Of the 61 CAA patients, 33 underwent a neuropsychological battery assessment. With the exception of one patient who was evaluated seven months before undergoing MRI, all the members of the cognitive onset CAA group underwent the neuropsychological assessment within four months of the MRI investigation. The neuropsychological battery included tests evaluating global cognitive efficiency (Mini-Mental State Examination, MMSE), memory (Verbal Span, Digit Span, Corsi Test, 15-Item Memory Test, Story Recall Test, Rey Complex Figure delayed recall), logical and executive functioning (Raven's Colored Matrices, Frontal Assessment Battery), attention (Trail Making Test A/B, Attentive Matrices, Stroop Test), language (Semantic and Phonemic fluency tests), and visuospatial perception (Rey Complex Figure copy). These examinations were performed by two experienced neuropsychologists.

2.2.3 Statistical analyses

Demographic and clinical characteristics and MRI markers were compared between the groups using the Kruskal–Wallis rank sum test for continuous variables and Pearson's Chi-squared tests for categorical variables, as appropriate. The Bonferroni correction was used to control for multiple comparisons in post-hoc analyses. The association between cognitive onset of CAA and all MRI markers was first assessed in separate univariate logistic regression models, after which a multivariate logistic regression model with backward stepwise selection of variables adjusted for age and sex was performed. To evaluate the relationship between location of CMBs and cognitive status, we performed a multivariate linear regression model adjusted for age and sex in the whole CAA study population and in the two groups (cognitive or hemorrhagic onset). Statistical computations were performed using R v. 3.5.3 (The R Foundation for Statistical Computing). Two-sided p-values <0.05 were considered to indicate

significance. Since the sample size was moderate, the p-values close to the threshold and in any case less than 0.1 was reported.

2.1 Results

2.1.1 Patient's characteristics

Table 4 lists demographic and clinical characteristics of the 61 eligible CAA patients, who were equally distributed between the two types of clinical presentation: 31/61 (50.8%) CAA presented with intracerebral hemorrhage at onset (age at onset 69.7 years; 42% females), and 30/61 (49.2%) with cognitive decline (age at onset 73.9 years; 53% females). The two study groups did not differ in terms of demographic characteristics, cerebrovascular risk factors or antiplatelet/anticoagulant medication consumption.

Applying the modified Boston criteria [32], 14 patients were diagnosed with possible CAA and 47 with probable CAA. Within the cognitive onset group, 4/30 (13.3%) patients received a diagnosis of possible CAA and 26/30 (86.7%) of probable CAA, while in the hemorrhagic onset group, 10/31 (32.3%) patients were diagnosed with possible CAA and 21/31 (67.7%) with probable CAA.

Table 4, Demographic and clinical characteristics of study subjects according to the clinical presentation at onset (cognitive vs hemorrhagic).

	Cognitive onset (n=30)	Hemorrhagic onset (n=31)	p value
Age at onset, mean±sd, y	73.9±8.6	69.7±11	0.15
Female, N. (%)	16 (53)	13 (42)	0.53
MMSE, mean±sd	19.5±6.2	24.3±4.5	0.32
Medical History			
Dyslipidemia, N. (%)	16 (53)	16 (52)	1
Hypertension, N. (%)	16 (53)	22 (71)	0.25
Diabetes mellitus, N. (%)	3 (10)	4 (13)	1
Smoking, N. (%)	11 (37)	10 (32)	0.92
Alcohol, N. (%)	10 (33)	11 (36)	1

Medications			
Warfarin, N. (%)	1 (3)	2 (7)	1
Aspirin, N. (%)	9 (30)	7 (23)	0.71
Statin, N. (%)	7 (23)	8 (26)	1

Kruskal–Wallis rank sum test and Pearson's Chi-squared tests

2.1.2 Associations of MRI markers

Association of MRI markers with cognitive onset CAA

The patients with cognitive onset CAA displayed a higher total amount of CMBs compared with those showing a hemorrhagic onset (p=0.000483). As regards location, only CMBs in the temporal and insular lobes were significantly more represented in the cognitive onset group (p=0.01505 and p=0.002001, respectively). The burden of WMHs was also greater in the patients with cognitive onset (p=0.01163) (Table 5). The univariate logistic regression analysis confirmed these associations and also showed a trend toward significance with MTA (p=0.0609) (Table 6). In a multivariate logistic regression model after adjustment for age and sex, the amount of CMBs was independently associated with cognitive disease onset (p=0.0282).

Table 5, MRI markers of small vessel disease and cortical atrophy in CAA patients with cognitive vs hemorrhagic onset.

	Cognitive onset (n=30)	Hemorrhagic onset (n=31)	p value
CMBs, N. (%) 0 1 2	 3 (10) 10 (33) 17 (57)	 17 (55) 8 (26) 6 (19)	 0.000483 ***
Frontal CMBs, N. (%)	23 (77)	16 (52)	0.07664
Temporal CMBs, N. (%)	20 (67)	10 (32)	0.01505 *
Insular CMBs, N. (%)	16 (53)	4 (13)	0.002001 **

Parietal CMBs, N. (%)	23 (77)	18 (58)	0.2025
Occipital CMBs, N. (%)	25 (83)	19 (61)	0.1022
Infratentorial CMBs, N. (%)	14 (47)	9 (29)	0.2475
cSS, N. (%) 0 1 2	 14 (47) 16 (53) 0	 19 (63) 11 (37) 0	 0.2634
cSS multifocality, N. (%) 0 1 2 3 4	 17 (57) 2 (7) 5 (17) 3 (10) 3 (10)	 19 (63) 5 (17) 3 (10) 3 (10) 0	 0.3179
WMHs, N. (%) 0 1 2 3	 0 5 (17) 17 (57) 8 (27)	 5 (16) 12 (39) 10 (32) 4 (13)	 0.01163 *
CSO-PVS, N. (%)	23 (77)	20 (67)	0.4226
BG-PVS, N. (%)	30 (100)	28 (93)	0.2173
Cortical microinfarcts, N. (%)	4 (16)	4 (16)	0.9634
MTA, N. (%) 0 1 2 3 4	 3 (10) 15 (50) 9 (30) 1 (3) 2 (7)	 6 (20) 19 (61) 5 (16) 1 (3) 0	 0.3311
GCA-F, N. (%)			

0 1 2 3	0 17 (57) 12 (40) 1 (3)	3 (10) 18 (58) 10 (32) 0	0.2412
PA, N. (%) 0 1 2 3	 3 (10) 9 (30) 15 (50) 3 (10)	 5 (16) 7 (23) 17 (55) 2 (6)	 0.787

BG-PVS, basal ganglia perivascular spaces; CMBs, cerebral microbleeds; CSO-PVS, centrum semiovale perivascular spaces; cSS, cortical superficial siderosis; GCA-F, global cortical atrophy-frontal; MTA, medial temporal lobe atrophy; PA, posterior atrophy; WMHs, white matter hyperintensities. * $p < 0.05$; ** $p < 0.01$; *** $p < 0.001$ Pearson's Chi-squared tests

Table 6, Association of MRI markers and CAA with cognitive onset.

	Estimate	p value
Univariate logistic regression		
CMBs	-1.3415	0.00038 ***
Temporal CMBs	-1.4351	0.00852 **
Insular CMBs	-2.0431	0.00164 **
WMHs	-1.0611	0.00409 **
MTA	-0.6479	0.0609
Multivariate logistic regression		
CMBs 1vs0	-1.52059	0.0648
CMBs 2vs1	-2.21080	0.0282*

CMBs, cerebral microbleeds; MTA, medial temporal lobe atrophy; WMHs, white matter hyperintensities. CMBs classes: 0 = 0 to 3 CMBs, 1 = 4 to 10 CMBs; 2 = more than 10 CMBs) * $p < 0.05$; ** $p < 0.01$; *** $p < 0.001$. The multivariate-stepwise logistic regression analysis was adjusted for age and sex

Association of MRI markers with MMSE score

In a multivariate linear regression model after adjustment for age and sex, cognitive impairment, as measured using the MMSE, was associated with CMBs in the insular lobe in the whole CAA population and with CMBs in the temporal lobe in the cognitive onset group (p=0.02555 and p=0.0206, respectively), and with CMBs in the occipital lobe in the hemorrhagic onset group (p=0.04782) (Table 7).

Table 7, Association of lobar CMBs location and cognitive status measured with MMSE score in the whole CAA study population and in the two groups of cognitive and hemorrhagic onset.

	Whole CAA population		Cognitive onset		Hemorrhagic onset	
	Estimate	p value	Estimate	p value	Estimate	p value
Frontal CMBs	6.25241	0.07567	1.1959	0.8448	3.59568	0.17646
Temporal CMBs	-6.01437	0.07488	-12.5249	0.0206*	-1.14513	0.49245
Insular CMBs	-5.57438	0.02555*	-1.8566	0.61	-1.35885	0.371
Parietal CMBs	-2.17174	0.60827	3.6592	0.5852	NA	NA
Occipital CMBs	3.08786	0.39389	6.2761	0.2492	-6	0.04782*
Infratentorial CMBs	5.69729	0.00607**	6.7413	0.0275*	0.55343	0.62342

CMBs, cerebral microbleeds; NA, not available, because the variable Parietal CMBs is strongly associated with the others, in particular with temporal and infratentorial CMBs ($p < 0.005$). * $p < 0.05$. The multivariate linear regression analysis was adjusted for age and sex

Association of MRI markers with CSF profile in cognitive onset CAA

Within the cognitive onset group, 16/30 patients underwent lumbar puncture. Interestingly, all patients showed indirect signs of cerebral amyloidosis, in terms of reduced values of CSF Aβ42 (14/16 patients) or borderline values of CSF Aβ42 together with altered Aβ42/p-tau and Aβ42/tau ratios (2/16 patients). Overall, 12 of the

16 (75%) patients with available CSF analysis showed AD-related tauopathy [60]. The presence of CSF AD pathology (amyloidosis and tauopathy) was not associated with any of the MRI markers considered.

Association of MRI markers with neuropsychological profile in cognitive onset CAA

Twenty-three of the 30 patients presenting with cognitive symptoms underwent a neuropsychological assessment. Seven of the 23 (30%) were classified as MCI and 16 (70%) as already having dementia. Overall, 16/23 (70%) patients exhibited a multidomain involvement, 4/23 (17%) a dysexecutive profile, and 3/23 (13%) an amnestic impairment. The total amount of CMBs did not differ among the neuropsychological profiles, whereas parietal lobe CMBs were significantly increased in patients with multidomain involvement versus those in the dysexecutive group (p=0.0316). Moreover, CMBs in temporal and insular lobes showed a tendency to be more expressed in patients with multidomain involvement compared with those in the amnestic group (p=0.0506 and p=0.0578, respectively). An increase in the Fazekas score was found in patients with multidomain involvement compared with those in the amnestic group (p=0.00413), and a trend toward significance was observed in the dysexecutive group compared with the amnestic group (p=0.05710) (Table 8).

Table 8, MRI markers of small vessel disease and cortical atrophy in CAA with cognitive onset according to neuropsychological profile.

	Multidomain (n=16)	Dysexecutive (n=4)	Amnestic (n=3)	p value
CMBs, N. (%) 0 1 2	 0 4 (25) 12 (75)	 1 (25) 1 (25) 2 (50)	 1 (33) 1 (33) 1 (33)	0.2292
Frontal CMBs, N. (%)	14 (88)	2 (50)	2 (67)	0.2325
Temporal CMBs, N. (%)	15 (94)	2 (50)	1 (33)	0.02135 *

Insular CMBs, N. (%)	11 (69)	2 (50)	0	0.08447
Parietal CMBs[a], N. (%)	16 (100)	2 (50)	2 (67)	0.01572 *
Occipital CMBs, N. (%)	15 (94)	3 (75)	2 (67)	0.3256
Infratentorial CMBs, N. (%)	8 (50)	3 (75)	0	0.1378
cSS, N. (%)				
0	8 (50)	2 (50)	0	0.2653
1	8 (50)	2 (50)	3 (100)	
2	0	0	0	
cSS multifocality, N. (%)				
0	10 (63)	2 (50)	1 (33)	0.6216
1	1 (6)	1 (25)	0	
2	2 (13)	1 (25)	1 (33)	
3	2 (13)	0	0	
4	1 (6)	0	1 (33)	
WMHs[b], N. (%)				
0	0	0	0	0.002077 **
1	1 (6)	0	3 (100)	
2	9 (56)	3 (75)	0	
3	6 (38)	1 (25)	0	
CSO-PVS, N. (%)	15 (94)	2 (50)	2 (67)	0.08744
BG-PVS, N. (%)	16 (100)	4 (100)	3 (100)	-
Cortical microinfarcts, N. (%)	2 (15)	0	0	0.7576

MTA, N. (%)				
0	3 (19)	0	0	0.2568
1	7 (44)	2 (50)	2 (67)	
2	5 (31)	2 (50)	0	
3	0	0	1 (33)	
4	1 (6)	0	0	
GCA-F, N. (%)				
0	0	0	0	0.9668
1	10 (63)	3 (75)	2 (67)	
2	5 (31)	1 (25)	1 (33)	
3	1 (6)	0	0	
PA, N. (%)				
0	1 (6)	1 (25)	0	0.4987
1	6 (38)	0	1 (33)	
2	7 (44)	3 (75)	1 (33)	
3	2 (15)	0	1 (33)	

BG-PVS, basal ganglia perivascular spaces; CMBs, cerebral microbleeds; CSO-PVS, centrum semiovale perivascular spaces; cSS, cortical superficial siderosis; GCA-F, global cortical atrophy-frontal; MTA, medial temporal lobe atrophy; PA, posterior atrophy; WMHs, white matter hyperintensities. * $p < 0.05$; ** $p < 0.01$ Pearson's Chi-squared tests. Pairwise comparisons: [a] Parietal CMBs: multidomain > dysexecutive ($p=0.0316$) patients; [b] WMHs: multidomain > amnestic ($p=0.00413$) patients

Chapter 3: Experimental Study 2

3.1 Aim

To describe the natural history and clinical-radiological outcomes following treatment for spontaneous CAA-ri.

3.2 Materials and Methods

3.2.1 Study design and participants

The study was designed as a multicenter, longitudinal observational study. Patients with first ever presentation of CAA-ri, diagnosed by clinical presentation, radiological criteria, and/or pathologic findings [24,25] were referred to the University of Milano-Bicocca within the iCAβ International Network [61] over a four-year period (2013 to 2017) (Figure 5). The initiative involved 35 neurology clinic hospitals, including the C. Mondino National Neurological Institute in Pavia, Italy. All patients were recruited from Neurology inpatients clinic wards. A predefined individual case-report form (CRF) for demographic, pathologic, clinical and medication history, clinical features, MRI images, exposure to immunosuppressive therapy, and clinical and radiological outcomes at follow-up has been systematically provided at time of each visit. The baseline CRF was provided at first-ever disease presentation and follow-up CRFs and MRI images were provided at each predefined visit at 3, 6, 12, 24-months and then annually. If multiple visits or MRI scans were performed for any clinical or therapeutic need, in addition to those suggested by the protocol, only the closest to the predefined time point was considered for the analyses. The patient inclusion criteria were: (1) available complete CRFs, (2) available adequate MRI images, and (3) at least one follow-up visit (including complete CRF and MRI images). Of the 150 consecutive patients, 11 did not meet diagnostic criteria for CAA-ri after centralized review (non-inflammatory CAA or other diseases) and 26 had no follow-up data; thus, 113 participants were eligible for the study. Diagnostic criteria for CAA-ri were centrally used by two expert neurologists to assign the diagnosis of 1) definitive (biopsy-proven), 2) probable (mono/multifocal, asymmetric, and bilateral WMH lesions suggestive of parenchymal VE and/or sulcal effusion, with or without leptomeningeal enhancement) or 3) possible (unilateral WMH lesions) CAA-ri.

Outcomes included survival, clinical and radiological recovery and CAA-ri relapse. Overall survival was defined as the time elapsed from the date of CAA-ri diagnosis to the date of death or last follow-up. Relapse-free survival was defined as the time elapsed from the date of ascertained clinical recovery to the date of the first subsequent clinical and radiological relapse, death or last follow-up available. Clinical recovery was defined as the stable recovery to neurological condition pre-existing to the acute inflammatory event, or the persistence of only the neurological deficits directly attributable to the brain vascular injury event (i.e. ICH), in the absence of new or worsened MRI findings. Given the lack of therapeutic recommendations, the choice of treatment was decided on a case-by-case basis by patients and their physicians. Radiological recovery was defined as the full resolution of the acute inflammatory WMH lesions suggestive of VE. Relapse of CAA-ri was defined as the presence of new-onset symptoms associated with MRI signs consistent with a new manifestation of CAA-ri, and only in participants with ascertained clinical and radiological recovery of the first presentation of the disease. A radiological progression without new symptoms was defined as an incomplete recovery.

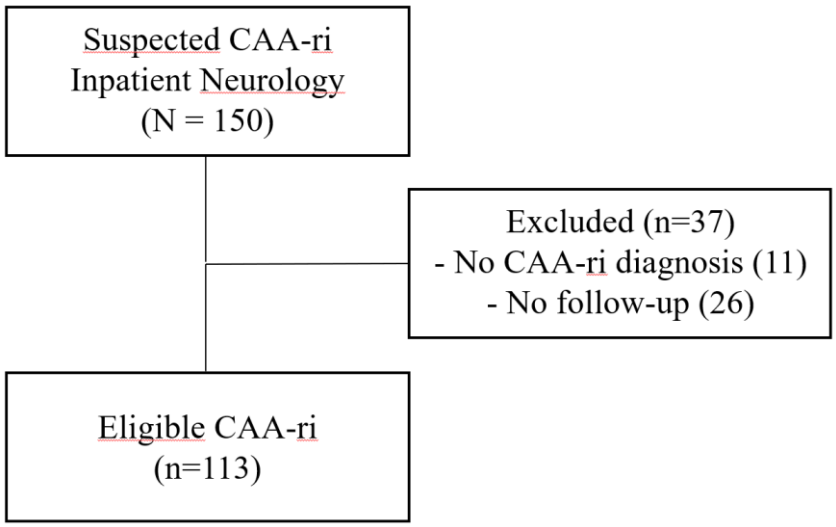

Figure 5 Flowchart illustrating the selection of the study participants. Study participants were selected from a larger study cohort (N=150), prospectively recruited at neurology clinic hospitals. Eleven participants did not meet diagnostic criteria for CAA-ri (non-inflammatory CAA or other diseases); 26 presented no follow-up data and were thus excluded.

3.2.2 Biomarkers

Neuroimaging

For the purposes of the study, the following MRI sequences were required: T1-weighted, GRE-T2*, fluid-suppressed T2-weighted (FLAIR). Additional MRI sequences were suggested: susceptibility-weighted imaging (SWI), T1 post-gadolinium sequences. All MRIs were acquired on 1.5-T imaging systems, according to routine clinical acquisition parameters used at each Centre. Visual reading of MRI images was centrally assessed by a trained neuroradiologist blinded to all clinical data and medical history.

MRI inflammatory manifestations were identified on the basis of patchy or confluent cortico-subcortical or deep WMH lesions suggestive of VE on FLAIR, with or without mass effect and with or without leptomeningeal involvement on T1 post-gadolinium sequences where available.

MRI CAA-related bleeding manifestations were based on acute brain MRI findings defined as presence of ≥1 of the following cortico-subcortical hemorrhagic lesions: CMBs (manual count), cSS (presence/absence), and ICH on T1-weighted and GRE-T2*.

3.2.3 Statistical analyses

Comparisons were obtained by using $\chi 2$ test or ANOVA for categorical and continuous variables, respectively. Overall survival and cumulative incidence/survival probability for clinical recovery, radiological recovery, and ICH were estimated using the Kaplan-Meier method. Concerning the analysis for clinical recovery, radiological recovery, and ICH, when the death event was observed in the absence of a previous event, the time to clinical recovery (or radiological recovery, and ICH) was considered censored at death time. Relapse-free survival was estimated from a 3-months landmark by the Simon-Makuch method in order to include the delayed entry of patients with clinical recovery over the entire follow-up. Analyses were performed using STATA 16.

3.3 Results

3.3.1 Patient's characteristics

Table 9 lists demographic and clinical characteristics at presentation of the 113 eligible patients with first ever diagnosis of CAA-ri. Twelve patients had a definite diagnosis of CAA-ri (10.6%), 81 probable (71.7%), and 20 possible (17.7%). The mean age of onset

was 72.9 years, 28.3% were less than seventy years, 43.4% were females. Previous history of MCI or AD dementia, and the radiological evidence of past ICH was 36.3% and 33.6%, respectively. The most frequent symptoms at presentation were cognitive or behavioral changes (71.7%) and focal neurological deficits (57.5%), followed by seizures (34.5%) and headache (22.1%). On MRI, 60.1% of patients had more than 10 CMBs, 47.8% had CMBs plus cSS, whereas 2.7% had only cSS. Positive gadolinium contrast-enhanced MRI was observed in 63.4% (see explanatory Figure 6).

The mean number of cases per center was 3, ranging from 1 to 16. Median follow-up time was 12 months. Overall follow-up at each time point was 100% at 3 months, 90.3% at 6 months, 69.9% at 12 months, and 29.2% at 24 months.

Table 9, Demographic and clinical characteristics at presentation of study subjects with diagnosis of CAA-ri.

	Definite CAA-ri	Probable CAA-ri	Possible CAA-ri	Total
N. (%) of patients	12 (10.6)	81 (71.7)	20 (17.7)	113 (100)
Female, N. (%)	4 (33.3)	35 (43.2)	10 (50.0)	49 (43.4)
Age at onset, mean (SD), y	70.9 (7.0)	73.9 (6.3)	70.2 (10.0)	72.9 (7.2)
< 70 y, N. (%)	4 (33.3)	18 (22.2)	10 (50.0)	32 (28.3)
History of N. (%)				
MCI or AD dementia	0 (0.0)	35 (43.2)	6 (30.0)	41 (36.3)
ICH	2 (16.7)	31 (38.3)	5 (25.0)	38 (33.6)
Symptoms onset, N. (%)				
Cognitive/Behavioral Changes	11 (91.7)	59 (72.8)	11 (55.0)	81 (71.7)
Focal Deficits	6 (50.0)	50 (61.7)	9 (45.0)	65 (57.5)
Seizures	2 (16.7)	29 (35.8)	8 (40.0)	39 (34.5)
Headache	5 (41.7)	16 (19.8)	4 (20.0)	25 (22.1)
Only 1 symptom	4 (33.3)	28 (34.6)	10 (50.0)	42 (37.2)
CMBs count, N. (%)				

None	1 (8,3)	2 (2,5)	-	3 (2.7)
1	-	7 (8.6)	1 (5.0)	8 (7.1)
2 - 4	1 (8.3)	4 (5,0)	5 (25.0)	10 (8.9)
5 - 10	4 (33.3)	18 (22.2)	2 (10.0)	24 (21.2)
>10	6 (50.0)	50 (61.7)	12 (60.0)	68 (60.1)
cSS, N. (%)	4 (33.3)	46 (56.8)	7 (35.0)	57 (50.4)
cSS+CMBs N. (%)	3 (25.0)	44 (54.3)	7 (35.0)	54 (47.8)
Gd contrast-enhanced MRI, N. (%)	7/9 (77.8)	46/69 (66.7)	6/15 (40.0)	59/93 (63.4)

AD, Alzheimer's disease; MCI, Mild Cognitive Impairment; ICH, Intracerebral hemorrhage; CMBs, cerebral microbleeds; cSS, cortical superficial siderosis; Gd, gadolinium.

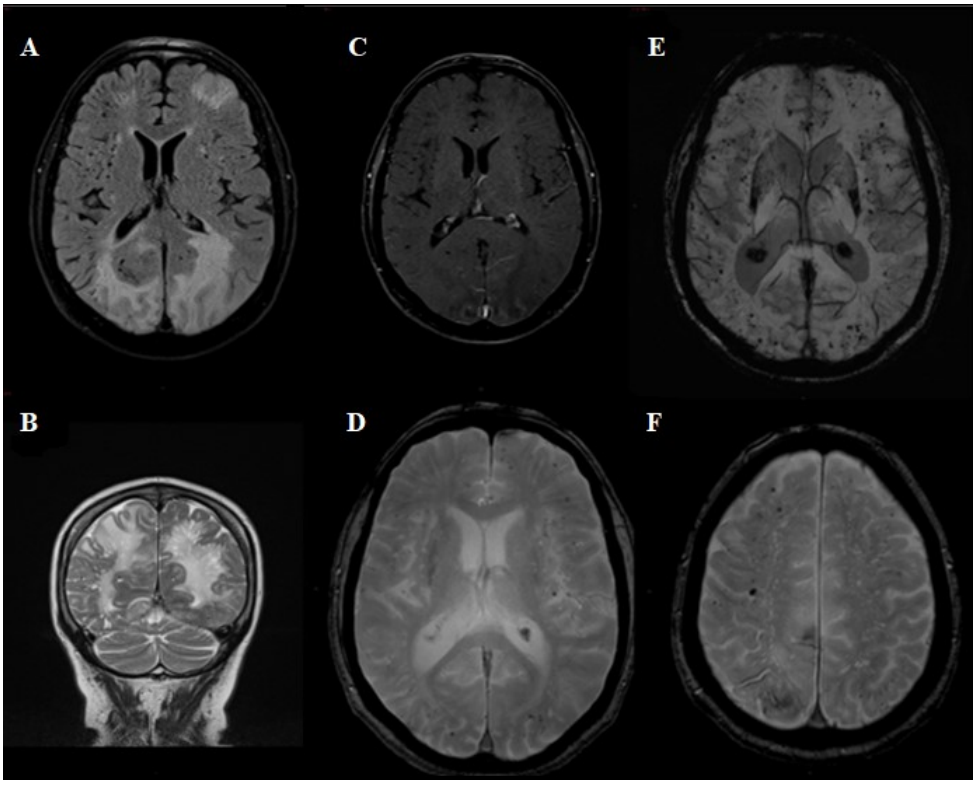

Figure 6 MRI features at the time of CAA-ri presentation. Prevalent posterior cortico-subcortical FLAIR hyperintensities (A, B). Posterior leptomeningeal enhancement post Gadolinium T1 image (C). Multiple cortical predominant microbleeds and superficial siderosis on GRE (D, E) and SWI (F) sequences.

3.3.2 Outcomes Evaluation at Follow-up

Survival

Overall survival and incidence probability of death are reported in Table 10. Thirteen patients died during follow-up: ICH (n=7), bronchopneumonia (n=3), cancer (n=1), status epilepticus (n=1), and unknown (n=1).

Table 10, Cumulative incidence probabilities of outcomes at 3, 6, 12, and 24-month follow-up in patients with diagnosis of CAA-ri.

	Incidence Probability, % (95% CI)				
Time point, mo	Death	Relapse	Clinical Recovery	Radiological Recovery	ICH Development
3	3.5 (1.3 - 9.2)	Landmark	70.3 (61.6 - 78.5)	45.1 (36.4 - 54.8)	7.1 (3.6 - 13.8)
6	5.5 (2.5 - 11.8)	6.9 (2.9 - 15.8)	80.2 (72.2 - 87.1)	59.3 (50.1 - 68.7)	9.2 (5.0 - 16.4)
12	11 (6.2 - 19.0)	16.2 (9.3 - 27.6)	84.1 (76.2 - 90.6)	77.4 (67.7 - 85.9)	11.9 (6.9 - 10.3)
24	18.6 (9.7 - 33.9)	38.3 (22.9 - 59.2)	84.1 (76.2 - 90.6)	77.4 (67.7 - 85.9)	17.1 (8.5 - 32.7)

ICH, Intracerebral hemorrhage. Cumulative incidence probability calculated from the beginning of the follow-up for death, clinical recovery, radiological recovery, and development of new ICH, by the Kaplan-Meier method. Cumulative incidence probability of relapse calculated from a 3-month landmark by the Simon-Makuch method in order to include the delayed entry of patients with clinical recovery over time. Clinical relapse defined as new-onset symptoms associated with new or worsening MRI findings at follow-up consistent with CAA-ri in participants with previously ascertained clinical recovery. In the case of multiple relapses, only the first relapse was considered.

Clinical and radiological recovery

The cumulative incidence probability of clinical and radiological recovery at 3, 6, 12, and 24-month follow-up is reported in Table 10.

The majority of patients showed a rapid clinical recovery within three months (70.3%; 95% CI, 61.6-78.5), with a further increase to 80.2% (95% CI, 72.2-87.1) and 84.1% (95% CI, 76.2-90.6) from three to six and from six to twelve months, respectively. The observed rate of radiological recovery was slightly slower compared to clinical recovery (45.1% vs 70.3% at three months; 59.3% vs 80.2% at six months follow-up). After one year, the cumulative incidence probabilities of radiological and clinical recovery were almost equal (77.4% and 84.1%, respectively). Figure 7 is indicative for a radiological recovery, while Figure 8 shows an incomplete radiological recovery.

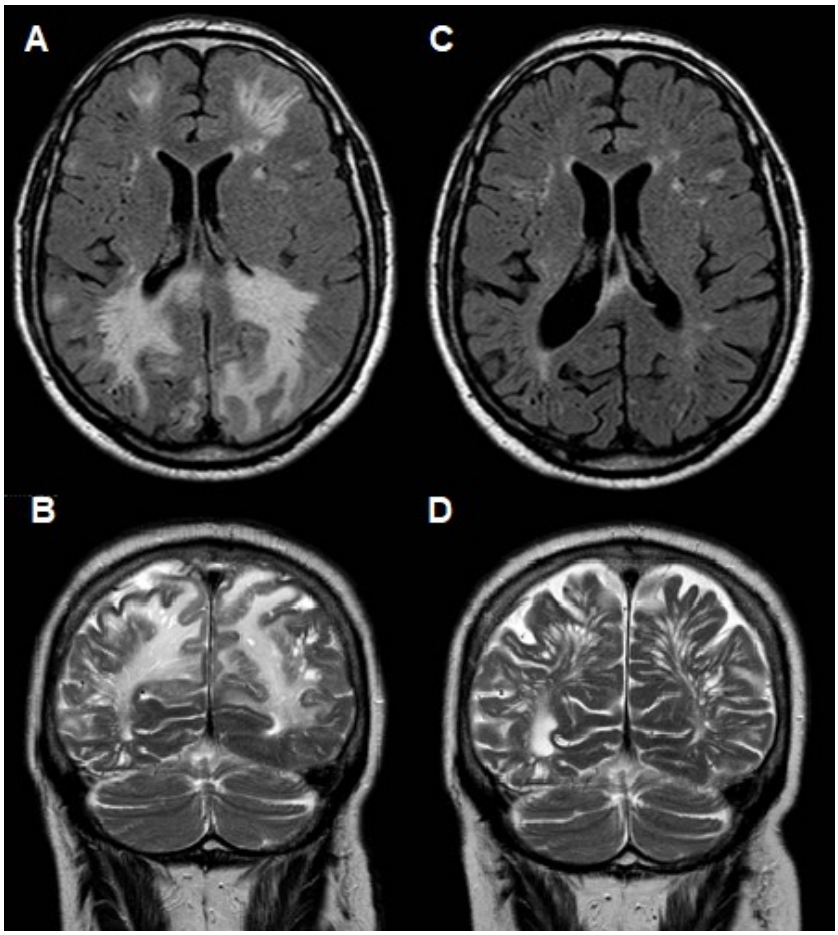

Figure 7 Relapse of CAA-ri with typical MRI evidence of white matter abnormalities on FLAIR sequences after steroid discontinuation (A, B), with radiological recovery after cyclophosphamide (C, D).

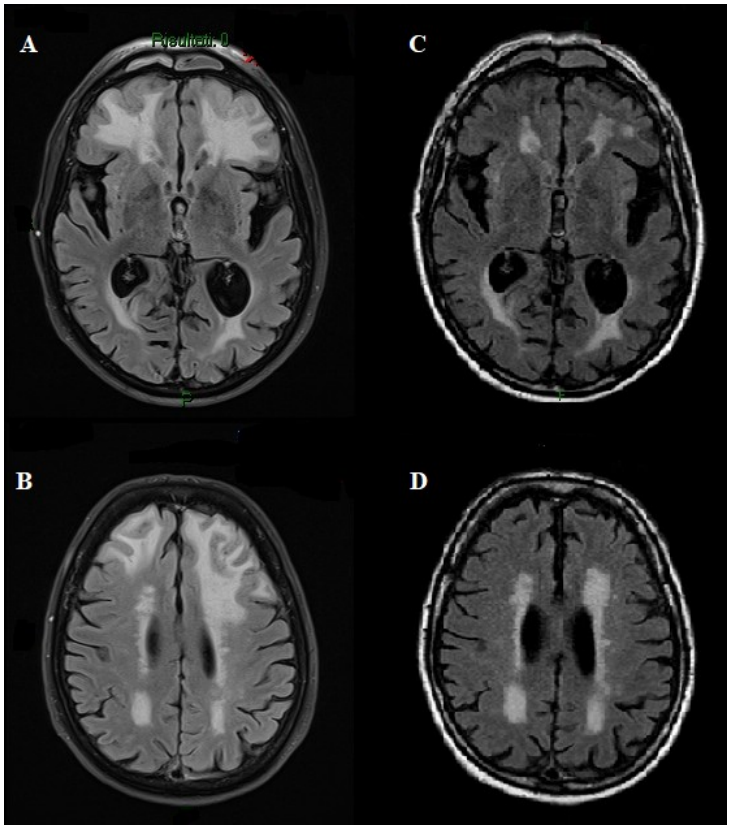

Figure 8 First presentation of CAA-ri with MRI evidence of white matter abnormalities on FLAIR sequences (A, B), with incomplete radiological recovery despite prolonged steroid treatment (C, D).

ICH

The observed incidence of acute ICH at follow-up are reported in Table 10. Overall, new ICH occurred in 13 patients, 8 of them (7.1%; 95% CI, 3.6-13.8) within the first three months.

Relapse and relapse-free survival

The observed probability of relapse was 6.9% (95% CI, 2.9-15.8) within six months, 16.2% (95% CI, 9.3-27.6) within twelve months, and 38.3% (95% CI, 22.9-59.2) within two years from the ascertained recovery of the first-ever presentation (Table 10). After 3 months from diagnosis (predefined landmark for recovery), fifteen of the 90 patients (16.7%) with clinical and radiological recovery had at least one CAA-ri relapse at follow-up.

Discussion

It is becoming increasingly evident that CAA is not a uniform, but rather a complex and very heterogeneous entity that can follow several different pathways [5]. Specific clinical phenotypes and imaging heterogeneity of the disease might be reflecting distinct neuropathological subtypes or patterns of cerebrovascular amyloid deposition and activation of diverging pathophysiological cascades [5]. Here we have explored the main clinical manifestations of the sporadic CAA. First, we focused on the disease onset, as a model to characterize the initial neuroradiological changes before the progression of the disease causes the diffuse and overlapping typical changes seen on MRI, focusing on the hemorrhagic and cognitive onset variant. Then, we explored the natural history, that is clinical and radiological episodes, of the emerging and increasingly recognized inflammatory variant.

In the first part of the study, in a clinically symptomatic cohort of patients with sporadic CAA, a higher burden of small vessel disease was detectable on brain MRI in CAA subjects with cognitive as opposed to hemorrhagic onset. Cognitive onset of CAA was indeed associated with an increased burden of WMHs and CMBs, and especially with the presence of CMBs in temporal and insular lobes. Our results expand the evidence that cognitive manifestation in CAA is associated with small vessel disease ischemic lesions and shed light to the still discussed role of the hemorrhagic alterations.

The association between cognitive onset CAA and WMHs is supported by previous solid evidence of a link between the presence of cognitive deficits and WMHs, both in the general population [40] and in CAA patients [44]. In CAA, vascular amyloid deposition, leading to loss of normal blood supply and ischemia, is a well-established contributor to white matter injury, while the contribution of degenerative mechanisms is still debated [62]. Nevertheless, the higher prevalence of WMHs in CAA with cognitive onset seems to suggest that these patients come to medical attention at a later stage of the disease. Furthermore, there is the possibility that the small vessel disease acts synergistically with an underlying neurodegenerative process in lowering the threshold for clinical cognitive manifestations.

CAA patients with cognitive onset displayed a higher total amount of lobar CMBs compared with the hemorrhagic onset group. The clinical significance of CMBs is still debated, some attributing to them a role as independent predictors, and others as

mediators of WMHs in the relationship between CMBs and cognition [40]. When CMBs are categorized as lobar, deep, and mixed, however, most of the evidence suggests a greater contribution to cognitive deficits of lobar versus deep ones [41,63–67]. As the pathogenesis of lobar CMBs commonly involves vessel wall damage due to CAA, also in the general population, in this study only lobar CMBs were considered. The effect of CMBs on cognition may be related directly to focal damage or to dysfunction of adjacent brain tissues; alternatively, CMBs may be a more general marker of severity of small vessel pathology [68]. An interesting finding of this study is the higher prevalence of CMBs in temporal and insular lobes in CAA with cognitive onset, supported by previous evidence that the relationship between lobar CMBs and poor cognitive performance was driven mainly by CMBs located in the temporal lobe [41]. It was suggested that the relationship between temporal CMBs and cognitive impairment could be explained, at least in part, by the higher number of CMBs in this lobe compared with other lobes found in a population-based setting [66]. In this CAA cohort this finding was not replicated; in addition, the severity of cognitive impairment, measured using the MMSE, was associated with CMBs in the insular and temporal lobes in the whole population and in the cognitive onset group respectively, but not in the patients with hemorrhagic onset.

To further investigate this finding, we analyzed small vessel disease markers according to CSF and neuropsychological profile. These analyses were conducted only within the cognitive onset group due to the lack of data availability in the hemorrhagic onset patients. In the cognitive onset group, all the patients showed indirect signs of cerebral amyloidosis, i.e., reduced values of CSF Aβ42 or altered Aβ42/p-tau and Aβ42/tau ratios, supported by previous evidence of an overlap between CAA and AD on CSF investigation [50]. In addition, CSF AD pathology, defined by decreased CSF Aβ42 together with increased tau or p-tau levels [60], was present in 75% of the cognitive onset cases, reinforcing the combined role of both CAA-mediated cerebrovascular and neurodegenerative alterations in the genesis of cognitive impairment. Neurodegeneration measured with tau-PET showed elevated uptake in AD regions in nearly half of a CAA-MCI cohort [69]; a lower percentage compared to the result of this study measured with CSF investigation, likely due to the prevalence of demented (70%) as opposed to MCI (30%) patients. The presence of CSF AD pathology was not

associated with any of the MRI markers considered, but this finding needs to be further investigated in a larger population taking advantage of different quantitative MRI markers.

In the cognitive onset group, neuropsychological assessment showed a prevalence of multidomain involvement (70%), followed by dysexecutive (17%) and amnestic (13%) patterns. Cognitive profile in CAA was originally attributed to dysexecutive impairment in non-demented patients [44,70]. Conversely, more than half of a CAA-MCI cohort showed an amnestic profile [69]. The multidomain involvement was prevalent in our cohort, likely due to the prevalence of overt dementia over MCI. Subjects with multidomain involvement displayed a greater burden of small vessel disease on MRI, in the form of WMHs and CMBs in the parietal lobe. Previously, unlike hippocampal volume and tau-PET binding, MRI markers of small vessel disease were not found to contribute to the presence of an amnestic versus non-amnestic profile in CAA-MCI subjects [69]. It is thus possible that when considering multidomain and more advanced cognitive profiles, the contribution of small vessel disease increases. The results of this study confirm the significant contribution of WMHs to cognitive impairment and reinforce the hypothesis that lobar location of CMBs may play a role.

The originality of this study consists in the subdivision of patients based on their CAA clinical onset. The main limitation, in turn, is the retrospective design, which limited the data availability on CSF and neuropsychological examinations. Moreover, CSF Aβ40 values were available only in a small number of patients, making it impossible to speculate reliably on this important biomarker. A further limitation is the inclusion of patients with possible CAA diagnosis, for which little MRI - pathological correlation has been performed [29]. Finally, the use of different MRI scanners (3T and 1.5T) is known to influence the detection of CMBs; in our case, however, CMB count was divided into categories to minimize the influence of single counts on the results.

The second part of the study, which included a longitudinal cohort of patients with a first diagnosis of CAA-ri, highlights the acute and transient, but potentially relapsing, inflammatory nature of the disease. The rate of radiological recovery was slightly slower compared to clinical recovery and at least one relapse occurred in 16.7% of the patients. These results suggest that spontaneous CAA-ri might be part of a broad

spectrum of Aβ-driven inflammatory processes, not only related to the use anti-Aβ antibodies administered for therapeutic purposes.

Most of the patients included in the study had some clinical manifestations of CAA, before CAA-ri presentation. A previous diagnosis of MCI/AD and ICH was present in 36% and 34%, respectively, to reflect the increased awareness on the clinical and radiological manifestations of spontaneous CAA-ri in the general neurology clinic setting and not only as ARIA-like events in AD clinical trials [71]. Although CAA-ri has been formerly reported as a severe presentation characterized by multiple clinical symptoms, it is noteworthy that 37% of this cohort presented with an isolated clinical manifestation. This raises the question of the under-recognition of CAA-ri episodes in the general population and in subjects with a previous history of MCI/AD or ICH at high risk for CAA-ri, particularly for very mild CAA-ri presentations that may be missed if not adequately investigated [72].

This cohort confirms the transient nature of the disease, with 70% and 80% of clinical recovery within 3 and 6 months, respectively, with a slightly slower rate of radiological recovery, that is 45% and 59% within 3 and 6 months, respectively. Therefore, it seems reasonable to base the therapeutic approach on the clinical picture rather than on the merely radiological presentation. A relatively small probability of early relapses was observed within 3 months; nevertheless the 38% of recurrences within 24 months highlights the importance to maintain a close follow-up in these patients, not to underestimate new neurological symptoms, and probably not to discontinue the immunomodulatory drugs too early [71].

The strengths of the study consist in the longitudinal and pre-defined protocol, with a central MRI reading. The main limitation consists in the lack of validated clinical-radiological guidelines. This could have influenced treatment decisions and interpretations of outcomes. The heterogeneity of patients and the lack of standard treatment, make it impossible treatments comparisons.

Conclusions

The results of these studies suggest that clinical and imaging heterogeneity of spontaneous CAA might be reflecting distinct phenotypes of the disease. Different neuropathological subtypes and patterns of cerebrovascular amyloid deposition have been demonstrated, i.e CAA type 2 (primarily haemorrhagic) and CAA type 1 (primarily expressed as cognitive decline), with many patients showing intermediate phenotypes of the disease. Diverging pathophysiological processes present peculiar MRI signatures, with WMHs being established associated with the development of cognitive decline, while CMBs presence and location needs further investigations to depict their role. The close relationship between vascular and plaque Aβ deposition, both conditions driven by impaired Aβ clearance, may superimpose a neurodegenerative AD-like process that mediates at least in part the cognitive impairment. CAA-ri is another probable intersection between CAA and AD, representing an overload of perivascular clearance pathways and the inflammatory effects of removing Aβ from CAA-positive vessels.

In conclusion, MRI markers as indirect signs of the underlying pathophysiological processes could provide relevant information on the CAA clinical spectrum. CAA-ri is a rare but frequently recurrent manifestation of CAA, which needs a prompt clinical-radiological identification for the potentially reversible condition.

References

1. Biffi A, Greenberg SM. Cerebral amyloid angiopathy: A systematic review. J Clin Neurol. 2011;7(1):1–9.
2. Viswanathan A, Greenberg SM. Cerebral amyloid angiopathy in the elderly. Ann Neurol. 2011;70(6):871–80.
3. Yamada M. Cerebral amyloid angiopathy: Emerging concepts. J Stroke. 2015;17(1):17–30.
4. Greenberg SM, Bacskai BJ, Hernandez-Guillamon M, Pruzin J, Sperling R, van Veluw SJ. Cerebral amyloid angiopathy and Alzheimer disease — one peptide, two pathways. Nat Rev Neurol. 2020;16(1):30–42.
5. Charidimou A, Boulouis G, Gurol ME, Ayata C, Bacskai BJ, Frosch MP, et al. Emerging concepts in sporadic cerebral amyloid angiopathy. Brain. 2017;140(7):1829–50.
6. Oppenheim G. Über “drusige Nekrosen” in der Grosshirnrinde. Neurol Cent. 1909;28:410–3.
7. Scholz W. StudienzurpathologiederhirngefabeII: die drusige entartung der hirnarterien und capillaren. Gesamte Neurol Psychiatr. 1938;162:694–715.
8. Pantelakis S. A particular type of senile angiopathy of the central nervous system: congophilic angiopathy, topography and frequency. Monatsschr Psychiatr Neurol. 1954;128:219–56.
9. Okazaki H, Reagan T, Campbell R. Clinicopathologic studies of primary cerebral amyloid angiopathy. Mayo Clin Proc. 1979;54:22–31.
10. Glenner GG, Wong CW. Alzheimer’s disease: Initial report of the purification and characterization of a novel cerebrovascular amyloid protein. Biochem Biophys Res Commun. 1984;120(3):885–90.
11. Greenberg SM, Vonsattel JPG, Stakes JW, Gruber M, Finklestein SP. The clinical spectrum of cerebral amyloid angiopathy: Presentations without lobar hemorrhage. Neurology. 1993;43(10):2073–9.
12. Keage HAD, Carare RO, Friedland RP, Ince PG, Love S, Nicoll JA, et al. Population studies of sporadic cerebral amyloid angiopathy and dementia: A systematic review. BMC Neurol. 2009;9:1–8.
13. Jellinger KA. Alzheimer disease and cerebrovascular pathology: An update. J

Neural Transm. 2002;109(5–6):813–36.

14. Ellis RJ, Olichney JM, Thal LJ, Mirra SS, Morris JC, Beekly D, et al. Cerebral amyloid angiopathy in the brains of patients with Alzheimers disease: The CERAD experience, part xv: CONCLUSION. Neurology. 1996;46(6):1592–6.
15. Sudlow C, Martínez González NA, Kim J, Clark C. Does Apolipoprotein E Genotype Influence the Risk of Ischemic Stroke, Intracerebral Hemorrhage, or Subarachnoid Hemorrhage? . Stroke. 2006;37(2):364–70.
16. Rostagno A, Holton JL, Lashley T, Revesz T, Ghiso J. Cerebral amyloidosis: amyloid subunits, mutants and phenotypes. 2010;67(4):581–600.
17. Bornebroek M, Haan J, Maat-Schieman MLC, Van Duinen SG, Roos RAC. Hereditary cerebral hemorrhage with amyloidosis-Dutch type (HCHWA-D): I - A review of clinical, radiologic and genetic aspects. Brain Pathol. 1996;6(2):111–4.
18. Bugiani O, Giaccone G, Rossi G, Mangieri M, Capobianco R, Morbin M, et al. Hereditary cerebral hemorrhage with amyloidosis associated with the E693K mutation of APP. Arch Neurol. 2010;67(8):987–95.
19. Herzig MC, Van Nostrand WE, Jucker M. Mechanism of cerebral beta-amyloid angiopathy: murine and cellular models. Brain Pathol. 2006;16(1):40–54.
20. Thal DR, Ghebremedhin E, Rüb U, Yamaguchi H, Del Tredici K, Braak H. Two types of sporadic cerebral amyloid angiopathy. J Neuropathol Exp Neurol. 2002;61(3):282–93.
21. Maia LF, Mackenzie IRA, Feldman HH. Clinical phenotypes of Cerebral Amyloid Angiopathy. J Neurol Sci. 2007;257(1–2):23–30.
22. Charidimou A, Martinez-Ramirez S, Shoamanesh A, Oliveira-Filho J, Frosch M, Vashkevich A, et al. Cerebral amyloid angiopathy with and without hemorrhage. Neurology. 2015;84(12):1206–12.
23. Eng JA, Frosch MP, Choi K, Rebeck GW, Greenberg SM. Clinical Manifestations of Cerebral Amyloid Angiopathy-Related Inflammation. Ann Neurol. 2004;55(2):250–6.
24. Chung KK, Anderson NE, Hutchinson D, Synek B, Barber PA. Cerebral amyloid angiopathy related inflammation: Three case reports and a review. J Neurol Neurosurg Psychiatry. 2011;82(1):20–6.

25. Auriel E, Charidimou A, Gurol EM, Ni J, Van Etten ES, Martinez-Ramirez S, et al. Validation of clinicoradiological criteria for the diagnosis of cerebral amyloid angiopathy-related inflammation. JAMA Neurol. 2016;73(2):197–202.
26. Sperling R, Salloway S, Brooks DJ, Tampieri D, Barakos J, Fox NC, et al. Amyloid-related imaging abnormalities in patients with Alzheimer's disease treated with bapineuzumab: a retrospective analysis. Lancet Neurol. 2012;11(3):241–9.
27. Piazza F, Greenberg SM, Savoiardo M, Gardinetti M, Chiapparini L, Raicher I, et al. Anti-amyloid β autoantibodies in cerebral amyloid angiopathy-related inflammation: Implications for amyloid-modifying therapies. Ann Neurol. 2013;73(4):449–58.
28. Charidimou A, Peeters A, Fox Z, Gregoire SM, Vandermeeren Y, Laloux P, et al. Spectrum of transient focal neurological episodes in cerebral amyloid angiopathy: Multicentre magnetic resonance imaging cohort study and meta-analysis. Stroke. 2012;43(9):2324–30.
29. Greenberg SM, Charidimou A. Diagnosis of cerebral amyloid angiopathy evolution of the Boston criteria. Stroke. 2018;49(2):491–7.
30. Greenberg SM, Rebeck GW, Vonsattel JP, Gomez-Isla T, Hyman BT. Apolipoprotein E epsilon 4 and cerebral hemorrhage associated with amyloid angiopathy. Ann Neurol. 1995;38(2):254–9.
31. Linn J, Halpin A, Demaerel P, Ruhland J, Giese AD, Dichgans M, et al. Prevalence of superficial siderosis in patients with cerebral amyloid angiopathy. Neurology. 2010;74(17):1346–50.
32. Knudsen KA, Rosand J, Karluk D, Greenberg SM. Clinical diagnosis of cerebral amyloid angiopathy: Validation of the boston criteria. Neurology. 2001;56(4):537–9.
33. Martinez-ramirez S, Romero J rafael, Shoamanesh A, Mckee AC, Van Etten E, Pontes-neto O, et al. Diagnostic value of lobar microbleeds in individuals without intracerebral hemorrhage. Alzheimers Dement. 2015;11(12):1480–8.
34. Charidimou A, Jäger HRJ. Developing biomarkers for cerebral amyloid angiopathy trials: Do potential disease phenotypes hold promise? Lancet Neurol. 2014;13(6):538–40.

35. Greenberg SM, Vernooij MW, Cordonnier C, Salman RA shahi, Edin F, Warach S, et al. Cerebral Microbleeds:A Field Guide to their Detection and Interpretation. Lancet Neurol. 2009;8(2):165–74.
36. Schrag M, McAuley G, Pomakian J, Jiffry A, Tung S, Mueller C, et al. Correlation of hypointensities in susceptibility-weighted images to tissue histology in dementia patients with cerebral amyloid angiopathy: A postmortem MRI study. Acta Neuropathol. 2010;119(3):291–302.
37. Martinez-Ramirez S, Greenberg SM, Viswanathan A. Cerebral microbleeds: Overview and implications in cognitive impairment. Alzheimer's Res Ther. 2014;6(3):1–7.
38. Vernooij MW, Van Der Lugt A, Ikram MA, Wielopolski PA, Niessen WJ, Hofman A, et al. Prevalence and risk factors of cerebral microbleeds: The Rotterdam Scan Study. Neurology. 2008;70(14):1208–14.
39. Chen S, Tsai H, Tsai L, Tang S, Lee B, Liu H, et al. Advances in cerebral amyloid angiopathy imaging. Ther Adv Neurol Disord. 2019;12:1–11.
40. Debette S, Schilling S, Duperron MG, Larsson SC, Markus HS. Clinical Significance of Magnetic Resonance Imaging Markers of Vascular Brain Injury: A Systematic Review and Meta-analysis. JAMA Neurol. 2019;76(1):81–94.
41. Li L, Wu DH, Li HQ, Tan L, Xu W, Dong Q, et al. Association of Cerebral Microbleeds with Cognitive Decline: A Longitudinal Study. J Alzheimer's Dis. 2020;75(2):571–9.
42. Linn J, Herms J, Dichgans M, Brückmann H, Fesl G, Freilinger T, et al. Subarachnoid hemosiderosis and superficial cortical hemosiderosis in cerebral amyloid angiopathy. Am J Neuroradiol. 2008;29(1):184–6.
43. Charidimou A, Linn J, Vernooij MW, Opherk C, Akoudad S, Baron JC, et al. Cortical superficial siderosis: Detection and clinical significance in cerebral amyloid angiopathy and related conditions. Brain. 2015;138(8):2126–39.
44. Case NF, Charlton A, Zwiers A, Batool S, McCreary CR, Hogan DB, et al. Cerebral Amyloid Angiopathy is Associated with Executive Dysfunction and Mild Cognitive Impairment. Stroke. 2016;47(8):2010–6.
45. Charidimou A, Meegahage R, Fox Z, Peeters A, Vandermeeren Y, Laloux P, et al. Enlarged perivascular spaces as a marker of underlying arteriopathy in

intracerebral haemorrhage: A multicentre MRI cohort study. J Neurol Neurosurg Psychiatry. 2013;84(6):624–9.

46. Charidimou A, Farid K, Baron JC. Amyloid-PET in sporadic cerebral amyloid angiopathy: A diagnostic accuracy meta-analysis. Neurology. 2017;89(14):1490–8.
47. Dondi F, Bertoli M, Lucchini S, Cerudelli E, Albano D, Bertagna F. PET imaging for the evaluation of cerebral amyloid angiopathy: a systematic review. Clin Transl Imaging. 2022;10(4):391–401.
48. Charidimou A, Farid K, Tsai HH, Tsai LK, Yen RF, Baron JC. Amyloid-PET burden and regional distribution in cerebral amyloid angiopathy: A systematic review and meta-analysis of biomarker performance. J Neurol Neurosurg Psychiatry. 2018;89(4):410–7.
49. Charidimou A, Friedrich JO, Greenberg SM, Viswanathan A. Core cerebrospinal fluid biomarker profile in cerebral amyloid angiopathy: A meta-analysis. Neurology. 2018;90(9):754–62.
50. Margraf NG, Jensen-Kondering U, Weiler C, Leypoldt F, Maetzler W, Philippen S, et al. Cerebrospinal Fluid Biomarkers in Cerebral Amyloid Angiopathy: New Data and Quantitative Meta-Analysis. Front Aging Neurosci. 2022;14(February):1–11.
51. Wardlaw JM, Smith EE, Biessels GJ, Cordonnier C, Fazekas F, Frayne R, et al. Neuroimaging standards for research into small vessel disease and its contribution to ageing and neurodegeneration. Lancet Neurol. 2013;12(8):822–38.
52. Gregoire S, Chaudhary U, Jager R, Brown M, Yousry T, Werring D. The Microbleed Anatomical Rating Scale (MARS): reliability of a tool to map brain microbleeds. Neurology. 2009;73(21):1759–66.
53. Charidimou A, Boulouis G, Roongpiboonsopit D, Auriel E, Pasi M, Haley K, et al. Cortical superficial siderosis multifocality in cerebral amyloid angiopathy: A prospective study. Neurology. 2017;89(21):2128–35.
54. Fazekas F, Chawluk JB, Alavi A. MR signal abnormalities at 1.5 T in Alzheimer's dementia and normal aging. Am J Neuroradiol. 1987;8(3):421–6.
55. Scheltens P, Leys D, Barkhof F, Huglo D, Weinstein HC, Vermersch P, et al. Atrophy of medial temporal lobes on MRI in "probable" Alzheimer's disease and

normal ageing: diagnostic value and neuropsychological correlates. J Neurol Neurosurg Psychiatry. 1992;55(10):967–72.

56. Koedam ELGE, Lehmann M, Van Der Flier WM, Scheltens P, Pijnenburg YAL, Fox N, et al. Visual assessment of posterior atrophy development of a MRI rating scale. Eur Radiol. 2011;21(12):2618–25.
57. Pasquier F, Leys D, Weerts J, Mounier-Vehier F, Barkhof F, Scheltens P. Inter- and intraobserver reproducibility of cerebral atrophy assessment on MRI scans with hemispheric infarcts. Eur Neurol. 1996;36(5):268–72.
58. Alcolea D, Pegueroles J, Muñoz L, Camacho V, López-Mora D, Fernández-León A, et al. Agreement of amyloid PET and CSF biomarkers for Alzheimer's disease on Lumipulse. Ann Clin Transl Neurol. 2019;6(9):1815–24.
59. Lewczuk P, Riederer P, O'Bryant SE, Verbeek MM, Dubois B, Visser PJ, et al. Cerebrospinal fluid and blood biomarkers for neurodegenerative dementias: An update of the Consensus of the Task Force on Biological Markers in Psychiatry of the World Federation of Societies of Biological Psychiatry. World J Biol Psychiatry. 2018;19(4):244–328.
60. Dubois B, Feldman HH, Jacova C, Hampel H, Molinuevo JL, Blennow K, et al. Advancing research diagnostic criteria for Alzheimer's disease: the IWG-2 criteria. Lancet Neurol. 2014;13(6):614–29.
61. The inflammatory Cerebral Amyloid Angiopathy and Alzheimer's disease Biomarkers International Network (iCAβ). Available at: https://sites.google.com/site/icabinternationalnetwork. Accessed May 8.
62. Graff-Radford J, Arenaza-Urquijo EM, Knopman DS, Schwarz CG, Brown RD, Rabinstein AA, et al. White matter hyperintensities: Relationship to amyloid and tau burden. Brain. 2019;142(8):2483–91.
63. Chung CP, Chou KH, Chen WT, Liu LK, Lee WJ, Chen LK, et al. Strictly Lobar Cerebral Microbleeds Are Associated with Cognitive Impairment. Stroke. 2016;47(10):2497–502.
64. Akoudad S, Wolters FJ, Viswanathan A, De Bruijn RF, Van Der Lugt A, Hofman A, et al. Association of cerebral microbleeds with cognitive decline and dementia. JAMA Neurol. 2016;73(8):934–43.
65. Gyanwali B, Shaik MA, Venketasubramanian N, Chen C, Hilal S. Mixed-

Location Cerebral Microbleeds: An Imaging Biomarker for Cerebrovascular Pathology in Cognitive Impairment and Dementia in an Asian Memory Clinic Population. J Alzheimer's Dis. 2019;71(4):1309–20.

66. Mesker DJ, Poels MMF, Ikram MA, Vernooij MW, Hofman A, Vrooman HA, et al. Lobar distribution of cerebral microbleeds: the Rotterdam Scan Study. 2011;68(5):656–9.
67. Meier IB, Gu Y, Guzman VA, Wiegman AF, Schupf N, Manly JJ, et al. Lobar microbleeds are associated with a decline in executive functioning in older adults. 2014;38(5):377–83.
68. Werring DJ, Gregoire SM, Cipolotti L. Cerebral microbleeds and vascular cognitive impairment. J Neurol Sci. 2010;299(1–2):131–5.
69. Schoemaker D, Charidimou A, Zanon Zotin MC, Raposo N, Johnson KA, Sanchez JS, et al. Association of Memory Impairment With Concomitant Tau Pathology in Patients With Cerebral Amyloid Angiopathy. Neurology. 2021;96(15):1975–86.
70. Xiong L, Davidsdottir S, Reijmer YD, Shoamanesh A, Roongpiboonsopit D, Thanprasertsuk S, et al. Cognitive Profile and its Association with Neuroimaging Markers of Non-Demented Cerebral Amyloid Angiopathy Patients in a Stroke Unit. J Alzheimer's Dis. 2016;52(1):171–8.
71. Antolini L, DiFrancesco JC, Zedde M, Basso G, Arighi A, Shima A, et al. Spontaneous ARIA-like Events in Cerebral Amyloid Angiopathy–Related Inflammation: A Multicenter Prospective Longitudinal Cohort Study. Neurology. 2021;97(18):1809-1822.
72. Banerjee G, Alvares D, Bowen J, Adams ME, Werring DJ. Minimally symptomatic cerebral amyloid angiopathy-related inflammation: Three descriptive case reports. J Neurol Neurosurg Psychiatry. 2019;90(1):113–5.

Acknoledgement

First, I would like to express my gratitude to Prof. Alfredo Costa for his continuous support in my career.

I am especially grateful to Lisa Farina for the MRI scans acquisition, to Elisabetta Zardini for the CSF immunoassay, to Sara Bernini for the neuropsychological assessment and to Elena Ballante for her support in the statistical analyses.

Finally, a warm thanks to Fabrizio Piazza for the precious collaboration within the iCAβ International Network.